Eur. Phys. J. D **11**, 247–256 (2000)

**THE EUROPEAN PHYSICAL JOURNAL D**

EDP Sciences


# Effects of solvation on dissociative electron attachment to methyl iodide clusters*

J.M. Weber[1,a], I.I. Fabrikant[1,2], E. Leber[1], M.-W. Ruf[1], and H. Hotop[1,b]

[1] Fachbereich Physik, Universität Kaiserslautern, 67663 Kaiserslautern, Germany
[2] Department of Physics and Astronomy, University of Nebraska, Lincoln, NE 68588-0111, USA

Received 29 November 1999 and Received in final form 14 January 2000

**Abstract.** Using laser photoelectron attachment to methyl iodide clusters in a differentially-pumped seeded supersonic helium beam and mass spectrometric ion detection, we have measured the rate coefficients for formation of $(CH_3I)_q{\cdot}I^-$ ($q = 0$–2) ions over the electron energy range 0–100 meV with an effective energy width of about 2.5 meV. Whereas a prominent vibrational Feshbach resonance just below the onset for the C–I stretch vibration ($\nu_3 = 1$) is observed for dissociative attachment to monomers (yielding $I^-$ ions), only weak and broad structure, shifted to lower energies, is detected for formation of $(CH_3I){\cdot}I^-$ ions and essentially no structure is left in the attachment spectrum for $(CH_3I)_2{\cdot}I^-$. These observations are interpreted by model $R$-matrix calculations which successfully describe the DA cross-section for the monomer and qualitatively recover the trend observed for cluster ion formation. For the clusters, the effects of increased electron-target long-range interaction and of solvation as well as coupling to soft vibrational modes lead to strong broadening and shifting of the vibrational Feshbach resonance and, ultimately, to its disappearance.

**PACS.** 34.80.Ht Dissociation and dissociative attachment by electron impact – 36.40.Qv Stability and fragmentation of clusters – 36.40.Wa Charged clusters

## 1 Introduction

One of the many interesting features of clusters is that they can serve as microscopic prototypes for studying the effects of solvation on the characteristics of both solvent and solvated particle, due to the interaction between a solvated molecule or ion and its surrounding solvent environment. Consequently, many cluster studies have been concerned with this topic in the past few years (for reviews see [1–6]), dealing with effects of both size and structure of the solvent cluster on, *e.g.*, vibrational transition energies, bond lengths, and electronic structure of the solvated species.

Solvation effects play also a key role in the formation of negative ions by attachment of slow electrons to clusters, a process that has received some attention lately [1,3]. Temporary negative ion states $XY^-$, formed in low energy electron collisions with molecules XY, have been found to be crucial for vibrational excitation as well as for formation of anions $X^-$ through dissociative attachment (DA) [1,3,7–11]:

$$e^-(\mathrm{E}) + \mathrm{XY} \rightarrow \mathrm{XY}^- \rightarrow \mathrm{X}^- + \mathrm{Y}. \qquad (1)$$

Well-known representatives of such temporary negative ion states are shape resonances (electrons trapped within a centrifugal barrier) and Feshbach resonances (electrons attached to electronically excited states $XY^*$ of the neutral molecule), in which the incoming electron is captured for a time interval long compared to the collision time and often similar to or even longer than a typical vibrational period. In special cases, if the combined long range interactions between a molecule or cluster and the incoming electron (predominantly electrical dipole and polarization forces) support a weakly bound state, resonances attached to vibrationally excited levels of the electronic ground state (called vibrational Feshbach resonances VFR) may occur. This type of resonances (previously addressed as "nuclear excited" Feshbach resonances [12,13]) has been discussed in detail by, *e.g.*, Domcke and Cederbaum [14] and by Gauyacq and Herzenberg [13]. In general, Feshbach resonances lie at energies below their neutral precursor; for vibrational Feshbach resonances one has thus to search at energies below the respective vibrationally excited XY ($\nu \geq 1$) levels. Experimental evidence for their existence has been provided some years ago for XY = HF in vibrationally inelastic electron scattering studies [15].

* Work based in part on chapter 7 of the unpublished doctoral dissertation of J.M. Weber (Fachbereich Physik, Universität Kaiserslautern, December 1998).

[a] *Present address*: Sterling Chemistry Laboratory, Yale University, P.O. Box 208107, New Haven, CT 06520-8107, USA.
[b] e-mail: `hotop@physik.uni-kl.de`

An especially clear example for a VFR was recently identified in a joint experimental and theoretical investigation of dissociative attachment to methyl iodide molecules at energies just below the onset for excitation of one quantum ($\nu_3 = 1$) of the C–I stretch vibration [16]; this VFR has been postulated before to play a role in the photochemistry of $I^-\cdot(CH_3I)$ cluster ions [17]. Subsequently, surprisingly sharp vibrational Feshbach resonances, associated with the intramolecular vibrations $\nu_2 = 1, 2$ and $\nu_3 = 1$, have been found in electron attachment to $N_2O$ clusters [18]; their widths ranged from 2.3 to 4.4 meV and the solvation shift (relative to the energies of the neutral clusters carrying intramolecular vibrational excitation) was small (redshift per added $N_2O$ unit about 0.7 meV). Similar, but broader VFRs (associated with the intramolecular vibrations $\nu_2 = 1, 2$ and $\nu_1 = 1$) were then detected in the yield for $(CO_2)_q^-$ cluster ion formation ($q \leq N$) from $(CO_2)_N$ clusters [19] with solvation shifts of about 12 meV per added $CO_2$ molecule.

For isolated molecules, DA normally proceeds through resonances which are repulsive at the internuclear distances of interest, *i.e.* in the Franck-Condon region associated with the vibrational ground state of XY. Correspondingly, the energy dependent DA cross-sections are characterized by broad bands up to several eV wide [3,7–9,11]. Resonances known from the molecular constituents are often major ion formation channels in DA to molecular clusters as well. However, the cluster environment will influence not only the resonance states themselves (*e.g.* shift the resonance position due to the effects of solvation), but can produce additional features which reflect the influence of the cluster environment on the resonance energy and symmetry [1]. One fascinating result in such studies of cluster anion formation is the observation of a strong resonance at zero energy in cases where such a feature is absent in the monomer (*e.g.* $O_2$ [20–22] and $H_2O$ [23,24]). In a recent investigation of $(O_2)_N$ clusters with monochromatized electrons (30 meV FWHM), Matejcik *et al.* [21,22] found – apart from a prominent, resolution-limited rise towards zero energy – peaks in the yield for $O_2^-$ and $(O_2)_2^-$ formation at higher electron energies which they ascribed to excited vibrational levels of the $O_2^-$ ion, solvated in clusters containing approximately 15 to 20 $O_2$ molecules, *i.e.* these peaks can be viewed as solvation-shifted levels of the $O_2^-(\Pi_g, v')$ shape resonance.

In DA of slow electrons to methyl iodide molecules [16,25], one observes a strong "zero-eV resonance", as well as a vibrational Feshbach resonance associated with the excitation of the first excited level of the C–I stretch vibration ($\nu_3 = 1$), peaking about 4 meV below the transition energy in the neutral molecule [16]. At the onsets for excitation of the $\nu_3 = 2$ and the $\nu_2 = 1$ vibrations ($\nu_2$ = symmetric $CH_3$ deformation) threshold cusps are visible in the DA cross-section due to the opening of these inelastic scattering channels. In pioneering work on DA to methyl iodide clusters, Klots and Compton [26] reported on the production of $(CH_3I)_q\cdot I^-$ ($q \geq 0$) ions in collisions of electrons of rather broad energy resolution (around 0.5 eV FWHM) with $CH_3I$ clusters. They derived a reaction scheme for the process by comparison of the DA results with electron impact ionization data (see Sect. 3.2).

Johnson and coworkers [6,17,27–29] as well as Arnold *et al.* [30] studied photodestruction of the $I^-\cdot CH_3I$ complex over the photon energy range from 3.3 to 3.6 eV. Their photoelectron spectra exhibit the same fine structure splitting as that of the bare $I^-$ ion, but shifted by $0.38 \pm 0.02$ eV to higher binding energies, consistent with the gas phase association enthalpy $\Delta H_a = 0.39 \pm 0.01$ eV of the complex [6,17,27–29], which can also be viewed as the solvation energy of the $I^-$ ion solvated at the $CH_3I$ molecule. The photoelectron spectra also show a progression of peaks due to the excitation of the C–I stretch vibration of the $I\cdot CH_3I$ complex upon photodetachment. Moreover, this group also investigated photofragmentation of the $I^-\cdot CH_3I$ complex, yielding $I^-$ ions [17]. Besides a prominent peak at threshold, their photofragmentation action spectrum exhibits two smaller peaks and a downward step slightly below the onset for excitation of the first, second and third quantum of the C–I stretch vibration, respectively. These features have been interpreted as vibrational Feshbach resonances, arising from inelastic scattering of the photoexcited excess electron from the $CH_3I$ molecule, while the iodine atom plays the role of a spectator [17]. We shall comment on this interpretation at a later stage.

In this combined experimental and theoretical study we present experimental data on the formation of $(CH_3I)_q\cdot I^-$ ($q = 0, 1, 2$) ions in DA to methyl iodide clusters at high electron energy resolution ($\Delta E \approx 2.5$ meV FWHM). The experimental results show a dramatic influence of the cluster environment on the vibrational Feshbach resonance observed in DA to methyl iodide molecules. We explain our findings on the basis of quasiclassical $R$-matrix calculations.

## 2 Experimental

Our experiment is based on the Laser Photoelectron Attachment (LPA) method, introduced by Klar *et al.* [31,32], and has briefly been described earlier in its present setup [18,24]: energy-variable, monoenergetic electrons are created by photoionization of atoms in a collimated beam; they interact with the target molecules (clusters) of interest in the region where the photoionization process takes place. Figure 1 shows a schematic view of the apparatus. Both hyperfine components of ground state $^{39}K(4s, F = 1, 2)$ atoms in a collimated beam of potassium atoms (collimation 1:400, diameter 1.5 mm) from a doubly differentially pumped metal vapor oven are transversely excited to the $^{39}K^*(4p_{3/2}, F = 2, 3)$ states by the two sidebands of an electro-optically modulated, stabilized CW Ti:sapphire laser ($\lambda_1 = 766.7$ nm, the excitation scheme is shown in Fig. 2). Part of the excited state population is transferred to high Rydberg levels ($nd$, $(n+2)s$, $n \geq 12$) or photoionized by interaction with the intracavity field of a broadband (40 GHz) tunable dye laser (power up to 5 W), operated in the blue spectral region

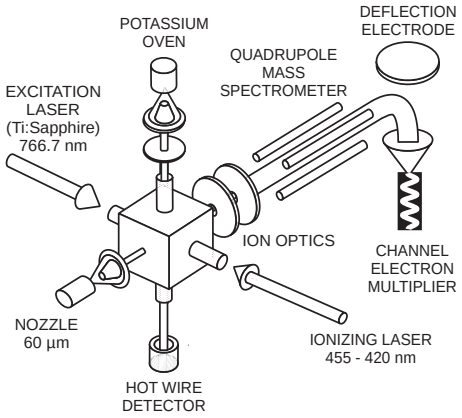


**Fig. 1.** Schematic view of the experimental setup.

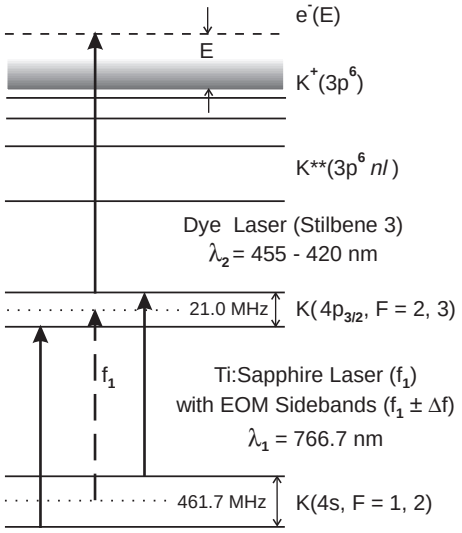


**Fig. 2.** Excitation scheme of the laser photoelectron attachment (LPA) experiment.

($\lambda_2$ = 472–424 nm, dye Stilbene 3). The energy of the photoelectrons can be continuously varied over the range 0–200 meV by tuning the wavelength of the ionizing laser ($\lambda_2 < 455$ nm).

Electrons, created in the overlap volume of the K atom and the laser beams, may attach to molecules and clusters in a collimated, differentially pumped nozzle beam (diameter in the reaction region 3 mm; nozzle diameter $d_0 = 60$ $\mu$m, stagnation pressure $p_0 = 3$ bar, nozzle temperature $T_0 = 33$ °C), propagating in a direction perpendicular to both the potassium and the laser beams. Anions, generated by electron attachment and drifting out of the essentially field free reaction chamber, are imaged into a quadrupole mass spectrometer ($m/q \leq 2\,000$ u/e) and detected by a differentially pumped off axis channel electron multiplier. For the sake of normalization and resolution testing, using the well known cross-section for $SF_6^-$ formation from $SF_6$, the target gas mixture contains 0.3% of $SF_6$ molecules. The gas mixture in the present experiment is prepared by flowing He gas (containing trace amounts of $SF_6$ as mentioned above) over a $CH_3I$ surface in a stainless steel container, which is kept at $T = 18$ °C,

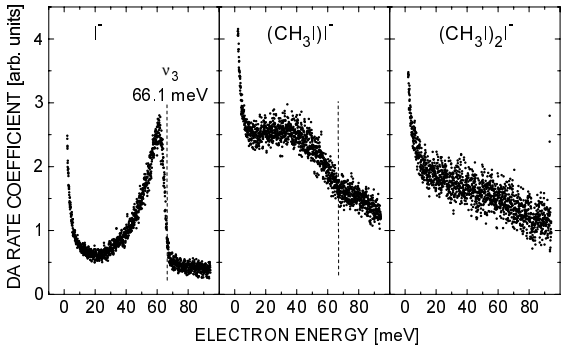


**Fig. 3.** Relative energy dependent rate coefficient $k_e(E)$ for the formation of $(CH_3I)_q{\cdot}I^-$ ions over the energy range 2–95 meV. The values have been normalized such that the corresponding ion yields amount to 100 for Rydberg electron transfer at very high principal quantum numbers ($n \approx 300$). The normalized ion yields have been multiplied by $E^{1/2}$ to obtain relative rate coefficients. The scatter of the data points represents the statistical $N^{1/2}$ error.

thereby saturating the carrier gas with $CH_3I$ vapor (partial pressure about 400 mbar). We note that the energy dependence of the rate coefficients for negative ion formation (see Fig. 3) was found to be independent of stagnation pressure over the range $p_0 = 0.4$ to 3 bar. Estimates show that laser-induced or collision-induced fragmentation (destruction) of product cluster ions is negligible under our experimental conditions.

The reaction volume is surrounded by a cubic chamber made of oxygen free, high conductivity copper, the inner walls of which are coated with colloidal graphite. By applying bias potentials to each face of the cube, DC stray electric fields are reduced to values $F_S \leq 70$ mV/m. Magnetic fields are reduced to values below 2 $\mu$T by compensation coils located outside the vacuum apparatus. The electron energy resolution is limited by the bandwidth of the ionizing laser ($\Delta E_L \approx 0.15$ meV), residual electric fields ($\Delta E_F \leq 0.25$ meV), the Doppler effect caused by the target velocity ($\Delta E_D \approx 0.07\sqrt{E}$, $\Delta E_D$ and electron energy $E$ in meV), and space charge effects due to $K^+$ photoions generated in the reaction volume (depending on the $K^+$ current). An upper limit to the overall energy spread close to $E = 0$ eV can be estimated by comparison of the $SF_6^-$ ion yield, measured under the same conditions as the cluster ion yield, with the cross-section measured by Klar *et al.* [31–33] at sub-meV resolution. In addition, the broadening of the sharp drop and of the cusp structure in the DA cross-section for $CH_3I$ [16] at the $\nu_3 = 1$ vibrational onset can be used for obtaining information on the effective energy width. For the present experiment at electron currents around 50 pA the overall resolution was estimated to be $\Delta E_{max} \approx 2.5$ meV.

## 3 Results and discussion

### 3.1 Experimental results

In DA of slow electrons to methyl iodide clusters only product ions of the composition $(CH_3I)_q{\cdot}I^-$ have been

observed. Figure 3 shows the energy dependent relative rate coefficients $k_e(E) = \sigma_e(E)v_e$ for the formation of $(CH_3I)_q{\cdot}I^-$ ions ($q = 0, 1, 2$) for electron energies $E = 2$–95 meV. At the lowest energies ($E < 10$ meV), a sharp "zero energy peak" is found in the cross-sections $\sigma_e(E)$, indicating $s$-wave threshold behaviour. In this energy range the cross-sections decrease more rapidly with rising energy than the function $E^{-1/2}$, leading to the decrease in the formation rate coefficients $k_e(E)$, observed in Figure 3 for all cluster sizes under study. The theoretical threshold law for $s$-wave capture involving long-range electron target interactions of the form $V(r) \propto r^{-m}$ ($m > 2$) demands $\sigma(E \to 0) \propto E^{-1/2}$ (in the absence of resonance states) [34]. As shown by Klar *et al.* [31] and Schramm *et al.* [33] for the molecule XY = $SF_6$ (for which $m = 4$), this behaviour is only reached at energies below 1 meV. For targets with permanent electric dipole moments ($m = 2$) as in the present case, a behaviour $\sigma(E) \propto E^{-x}$ with $x$ in the range 0.5–1 can be expected at "low" energies [35,36]; rotation has to be included (and experimentally resolved) to make more detailed predictions. Figure 3 does not include the limiting range $E \to 0$ and therefore does not allow statements on the threshold law. At higher electron energies the energy dependence of the relative rate coefficients is strongly dependent on the size of the formed cluster ions. In the rate coefficient for the formation of $I^-$ we find a pronounced peak slightly below the onset for the excitation of the C–I stretch vibration ($\nu_3$). This peak has recently been reported in an experiment on DA to thermal $CH_3I$ molecules ($T_G = 300$ K) by Schramm *et al.* [16,37], and has been identified as a vibrational Feshbach resonance [16]. In the formation rate coefficient for $CH_3I{\cdot}I^-$ ions this resonance is reduced to a broad shoulder at lower energies, and for $(CH_3I)_2{\cdot}I^-$ the structure has vanished (see Fig. 3).

### 3.2 Basic considerations on the dynamics of DA to $CH_3I$ clusters

In order to gain a first understanding of the observed dramatic change in the energy dependent rate coefficients for $(CH_3I)_q{\cdot}I^-$ cluster ion formation ($q = 0$–2) we will look at the repulsive ionic potential energy curve relevant for the DA process in relation to that of the neutral potential curve for the case of a single molecule (see Fig. 4) (the methyl iodide molecule offers a prototype for weak excess electron binding through combined dipole and polarization forces) and compare the situation with that of DA to a cluster. We shall treat the $CH_3I$ molecule as "quasi-diatomic", taking into account only the potential energy as a function of the C–I internuclear distance $\rho_1$, thereby neglecting the internal structure of the $CH_3$ group, as well as the possibility of energy transfer into internal degrees of freedom of the methyl radical upon dissociation (*e.g.* excitation of the umbrella mode). The assumption of this "rigid radical limit" is a good approximation, as essentially the full exothermicity of the dissociation process (0.62 eV) appears as translational energy of the products, according

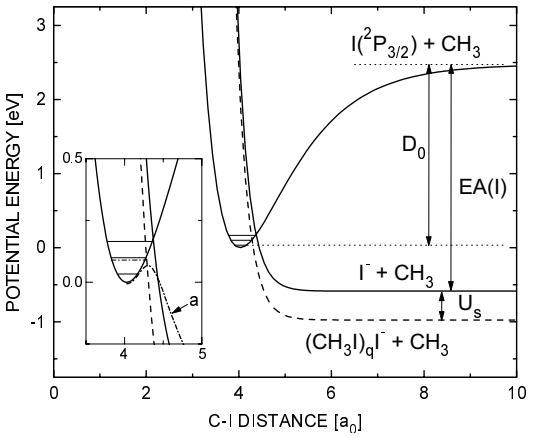


**Fig. 4.** Potential energy curves for dissociative electron attachment involving the methyl iodide molecule. The dashed curve represents an ionic potential down-shifted by $U_S$ due to the solvation effect, as relevant for clusters (in the figure we use $U_S = 0.39$ eV, as relevant for the dimer, $q = 1$). In the insert, the region of the curve crossing is shown enlarged, including the adiabatic molecular negative ion curve (dash-dotted line, "a") and the level of the $\nu_3 = 1$ vibrational Feshbach resonance (horizontal dash-dotted line).

to measurements of the kinetic energy release upon DA following Rydberg electron transfer to $CH_3I$ and $CD_3I$ [38]. Most of the energy is carried away by the neutral $CH_3$ fragment, while the heavier $I^-$ ion receives only about 63 meV. To model the process we use the potential energy curves already successfully applied to the problem in [16]. The potential curve of the neutral molecule is parameterized by a Morse potential

$$V(\rho_1) = D_e[1 - \exp\big(-\beta(\rho_1 - \rho_e)\big)]^2 \qquad (2)$$

where the parameters are chosen to reproduce the experimental values for the dissociation energy $D_0 = 2.44$ eV [39], the equilibrium C–I internuclear distance $\rho_e = 4.029a_0$ [40], and the (0–1) spacing of the $\nu_3$ vibration (C–I stretch, 66.1 meV [41], $\beta = 0.9029a_0^{-1}$). The repulsive negative ion curve is represented by

$$U(\rho_1) = B\exp\big(-b(\rho_1 - \rho_e)\big) + C \qquad (3)$$

using $C = -0.587$ eV in accord with the experimental value of 0.62 eV for the exothermicity of the process (*i.e.* the energy difference between the electron affinity of $I(^2P_{3/2})$, 3.059 eV [42], and the dissociation energy of $CH_3I$, $D_0 = 2.44$ eV). The fit parameters $B = 2.993$ eV and $b = 3.992a_0^{-1}$ are chosen to optimize the energy value and slope of the negative ion curve $U(\rho_1)$ in the region of the crossing with the neutral potential $V(\rho_1)$ [16]. Taking into account the long range dipolar and polarization forces ($\mu_d = 1.62$ Debye, $\alpha = 54a_0^3$) and using a reasonable dependence of $\mu_d$ and $\alpha$ on the internuclear distance $\rho_1$ [43] quasi-classical $R$-matrix calculations on DA to single methyl iodide molecules exhibit very good agreement with the experimental data of Schramm *et al.* [16].

The main differences between DA to single $CH_3I$ molecules and to $(CH_3I)_N$ clusters are:

(i) In a $(CH_3I)_q{\cdot}I^-$ ion ($q \geq 1$) the $I^-$ will be solvated by the residual cluster constituents, resulting in a downward shift of the negative ion curve by the amount of the vertical solvation energy $U_S$, as indicated by the dashed line shown in Figure 4. In order to assist the mind's eye (see insert in Fig. 4), we will now view the DA process in terms of an avoided crossing of two potential curves as a function of the C–I distance of the dissociating molecule, one describing the excess electron loosely bound to a neutral methyl iodide molecule (*i.e.* the curve runs parallel to and close below that of the neutral molecule), the other one describing the repulsive state after the collapse of the excess electron's wave function into the antibonding $\sigma^*$ orbital, finally leading to the formation of a neutral methyl radical and a $I^-$ ion. This adiabatic view yields a potential well at small internuclear distances, separated from the dominantly repulsive behaviour at larger distances by a barrier that gives rise to the existence of vibrational states of the negative ion, in other words, vibrational Feshbach resonances. If the repulsive curve is lowered in energy due to solvation of the $I^-$ ion by the molecules of the cluster, this potential well will become smaller, until it no more supports the existence of bound states (vibrational Feshbach resonances). Qualitatively, this will lead to the disappearance of the structure in the DA cross-section assigned to the vibrational Feshbach resonance. We stress the fact that this simple adiabatic picture is only inferred to visualize the situation and should be viewed with caution as the coupling of electronic and nuclear motion, which is one of the key properties of a vibrational Feshbach resonance, renders such an adiabatic view inappropriate to describe the process correctly.

(ii) The total dipole moment and polarizability of the target influencing the incoming electron will be that of the whole cluster. While the polarizability of the cluster may be estimated using integer multiples of the molecular polarizability, the total dipole moment will be strongly dependent on the structure of the cluster.

(iii) Part of the exothermicity of the DA process may be distributed into soft intermolecular vibrational modes of the $(CH_3I)_{N-1}{\cdot}I^-$ ion formed immediately upon dissociation. These soft modes are expected to wash out the sharp threshold cusps observed by Schramm *et al.* [16] at the onsets for the excitation of the C–I stretch vibration, and the $R$-matrix calculations discussed below corroborate this expectation. Energy redistribution among intermolecular degrees of freedom will not only affect the overall DA cross-section, but may as well lead to evaporation of monomers until a stable configuration with $q \leq N-1$ constituents is reached. Further monomer evaporation may take place while the cluster is regrouped into an energetically more favorable geometry. Klots and Compton [26] used an electron beam with rather poor resolution in studies on electron attachment to methyl iodide clusters. They observed exclusively ions of the type $(CH_3I)_q{\cdot}I^-$ ($q \geq 0$), *i.e.* products of a dissociative attachment process, and found the intensities of $(CH_3I)_q{\cdot}I^-$ (generated at low electron energies) and of $(CH_3I)^+_{q+1}$ (produced in electron impact ionization of $(CH_3I)_N$ clusters) to be correlated. From this they concluded that the DA process should have the form

$$(CH_3I)_{q+1} + e^- \rightarrow (CH_3I)_q{\cdot}I^- + CH_3. \qquad (4)$$

This reaction scheme implies that the clusters do not fragment upon electron impact ionization. We note that this is not necessarily the only possible conclusion to be drawn from the mentioned correlation of DA and electron impact data. One could observe the same correlation if the $(CH_3I)^+_{q+1}$ cations and the $(CH_3I)_q{\cdot}I^-$ anions just had identical neutral precursers, regardless of their size. On the other hand, due to the mass ratio of the DA products (cluster ion and $CH_3$ radical) most of the excess energy will reside on the light, ejected methyl radical; correspondingly, fragmentation (monomer evaporation) seems unlikely, especially for DA to the methyl iodide dimer. We therefore adopt reaction scheme (4) for the cases of interest ($q = 0$–$2$), and we use it along semiclassical $R$-matrix theory to calculate the cross-section for the formation of $CH_3I{\cdot}I^-$ ions.

Unlike in the case of DA to a single molecule, where the symmetry of the DA process along the C–I bond axis prevents change of angular momentum of the nuclear wave function, rotational excitation may occur in DA to clusters, as the symmetry is broken by the cluster environment of the dissociating molecule. This rotational excitation may be accompanied by vibrational excitation of the I–I stretching mode. To find the energy distribution among all these degrees of freedom, one needs a complete analysis of vibrational and rotational modes of the complex and couplings between them. On the other hand, these effects should not be very strong: due to the large mass difference (15 u for $CH_3$ and 269 u for the residue) almost all released energy goes into motion of the $CH_3$ radical which is emitted from the dissociating molecule far from its planar equilibrium structure and can therefore be expected to carry some vibrational energy after dissociation. In addition, the rotational-vibrational distribution of the fragments may be considered as a postcollisional effect not affecting the dynamics of the primary DA process with formation of $CH_3$. Therefore, our theoretical treatment of the problem will focus on the electron scattering channels and their interaction with the DA channel leading to formation of the vibrational Feshbach resonance (VFR).

In this context, a comment on the interpretation of photodestruction of $I^-{\cdot}CH_3I$ complexes by Dessent *et al.* [17] seems appropriate. These authors had observed structure in the $I^-$ photofragment action spectrum at about 60 meV above the photodestruction onset for this system. Led by the results of Hotop *et al.* [37], who had reported a sharp asymmetric resonance structure below the $\nu_3 = 1$ onset in DA to free methyl iodide molecules (interpreted in [17] to be a VFR), Dessent *et al.* assumed that this VFR was also active in their system. In other words, they attributed this structure to photoexcitation of the $I^-{\cdot}CH_3I$ ion-molecule complex into a state, where the excess electron is trapped in a weakly-bound, diffuse state

within the electrostatic field of the vibrationally excited $I{\cdot}CH_3I$ complex. We note that the slightly misleading term "half-collision", used in [17], does not mean that the excess electron is actually scattered from the $CH_3I$ molecule in the complex, but that a state similar to one populated in the closest approach of a scattering experiment is excited. While this state is of the same fabric as the VFR observed in DA to the bare $CH_3I$ molecule [16,37], the mode of populating this state will lead to a different time evolution of the total wave function of the system in the two experimental approaches due to the non-adiabatic nature of the coupling of the weakly bound VFR state to the continua of DA and of autodetachment. The precise nature of the structure below each of the $\nu_3 \geq 2$ onsets in the $I^-$ photoaction spectrum in [17] is ambiguous. If the relevant potential curves for the $I^-{\cdot}CH_3I$ ion-molecule complex were the same as for the bare $CH_3I$ molecule, the structures associated with $\nu_3 = 2$ cannot be due to VFR excitation, as the location of the crossing of the neutral and the DA curves does not support a VFR for any vibrational state above $\nu_3 = 1$. On the other hand, the modified potential curve, appropriate to the process observed by Dessent *et al.* [17], could allow a VFR to exist for $\nu_3 = 2$. The states observed by Dessent *et al.* above allowed VFR levels could be described as predissociating dipole bound vibrational states, but require a full non-adiabatic theoretical treatment for detailed understanding. Concluding the comparison between the photoexcitation approach using the ion-molecule complex described in [17] and the DA experiment to the bare molecule ([16,37] and the present work), the basic paradigm for the structures associated with the $\nu_3 = 1$ state is probably the same, namely the existence of a VFR, while the higher vibrational states have to be described differently. While the additional I atom in the photoexcited complex does not change this paradigm, its role is certainly not restricted to that of a spectator, as the long-range forces of the complex are clearly modified by the presence of the I atom, thus changing the relative positions of the potential curves. Moreover, it introduces soft modes not present in the bare molecule.

### 3.3 R-matrix theory of electron attachment to methyl iodide clusters

We will assume that the basic physics of the process of attachment to the cluster can be described in terms of attachment to an individual molecule. However, both stages of this process, electron capture and dissociation, are strongly influenced by the interaction of the incident electron and the dissociating monomer with the environment. We apply the resonance $R$-matrix theory essentially in the same way as we did for the monomer [16]. The whole space is divided into two regions, namely inside and outside the $R$-matrix sphere. Outside the $R$-matrix sphere the electron-cluster interaction can be described in terms of the dipolar and polarization forces. According to calculations of Wang *et al.* [44], the iodine atoms in the equilibrium configuration of the $(CH_3I)_2$ dimer stand head-on

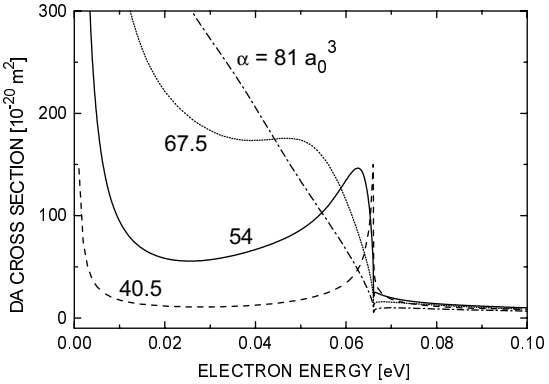


**Fig. 5.** Calculated cross-sections for dissociative electron attachment to (model) $CH_3I$ monomers with different polarizabilities $\alpha$ (potential energy curves and dipole moment fixed) to illustrate the strong influence of the long-range electron molecule interaction (here polarization potential) on the vibrational Feshbach resonance appearing just below the $\nu_3 = 1$ threshold.

each other at a distance of about 0.3 nm, the dipole moments having an angle of 120°, so that the dipole moment of the dimer is the same as for the monomer. We note here that calculations by Ehbrecht *et al.* [45] on $(CH_3F)_2$ yielded a structure with antiparallel C–F axes, the dipole moments of the two $CH_3F$ molecules thereby compensating each other. In the case of $(CH_3I)_2$, the I–I interaction appears to play a more important role than the interaction energy of the two molecular dipoles. It is conceivable, however, that the global minimum structure determined by Wang *et al.* [44] is not the only possible scenario and that the barriers between the global minimum of the potential surface and local minima are small. We note that recent SCF/MP2 calculations of the methyl iodide dimer structure by Gallup [46] qualitatively confirm the results of Wang *et al.* [44], but give more local minima (in particular for head-to-tail geometry).

Regarding polarizability, we can assume that the dimer has just double the polarizability of the monomer, and we account for this by adding a distant-independent term to the polarizability function $\alpha(\rho)$ used in [16]. In order to see how a variation of the polarizability $\alpha$ changes the shape and the structure of the cross-section, we have performed several calculations for the monomer with different values of $\alpha$. The results, presented in Figure 5, reveal that a relatively small change in $\alpha$ leads to a drastic change in the cross-section. In particular the vibrational Feshbach resonance is strongly affected, as illustrated by the result obtained for $\alpha = 81$ au. For smaller $\alpha$, on the other hand, the resonance moves closer to the vibrational threshold and crosses it eventually (becoming a virtual state), as demonstrated for $\alpha = 40.5$ au. For dimers, however, a simple form of the polarization interaction outside the $R$-matrix sphere of radius $r_0 = 5a_0$, $V_{\rm pol} = -e^2\alpha/2r^4$, used in our monomer calculations, cannot be adopted: due to the relatively large size of the dimers the asymptotic form of the potential is not yet reached just outside the $R$-matrix sphere. To account for this, we will assume that

each $CH_3I$ monomer creates a polarization well with a constant potential $-e^2\alpha/2r_0^4$ at $r < r_0$. Since the intermediate resonance negative-ion state is dominated by the $s$-wave, we can calculate the effective electron-dimer interaction outside the $R$-matrix sphere by averaging the double-well interaction over all orientations of the dimer with respect to the radius vector of the electron.

Again using a simple model, we also estimated the solvation energy $U_S$ of the $CH_3I$–$CH_3I^-$ complex as a function of the distance between the centers of the $CH_3I$ and $CH_3I^-$ constituents (assumed to be both spherically symmetric). This was achieved by averaging the interaction between a point charge and a monomer, placed at distance $R$ from the center, over the $R$-matrix sphere. Within the range $5a_0 < R < 8a_0$ the resulting energy $U_S$ can be expressed by

$$-U_S = 1.50664 - 0.20152R + 0.005587R^2$$

($R$ in $a_0$, $U_S$ in eV). When evaluated at the I–I distance of the ground state dimer ($R = 0.3$ nm $= 5.67a_0$) [44], one obtains $U_S = -0.54$ eV. A more realistic distance should be somewhat larger; in fact, the experimentally determined value $U_S = -0.39$ eV [6,17] corresponds to $R = 6.75a_0$. Variation of $R$ in that range leads to very little change in our results for cross-sections.

The electron wave function outside the sphere is matched with the internal wavefunction using the $R$-matrix as a function of the distance $\rho_1$ between the C and I nuclei in the one-pole approximation

$$R(\rho_1) = \frac{\gamma^2(\rho_1)}{W(\rho_1) - E} + R_b \qquad (5)$$

where $R_b$ is a background term weakly dependent on $\rho_1$, and $W(\rho_1)$ is the lowest $R$-matrix pole which can be related to the potential energy curve of the neutral molecule $V(\rho_1)$ and the negative-ion diabatic curve $U(\rho_1)$ by the simple relation

$$W(\rho_1) = U(\rho_1) - V(\rho_1). \qquad (6)$$

We will assume that at $r < r_0$ the electron interaction with the environment leads to a constant negative correction $U_S = -0.39$ eV (solvation energy discussed above). Generally this correction depends on the nuclear coordinates, but in first approximation it is reasonable to neglect this dependence. Then the parameter $W$ is also shifted by $U_S$, and the parameter $\gamma$ does not change at all.

In Figure 6 we present DA cross-sections relevant for the dimers, as calculated with the polarization potential discussed above and different solvation energies $U_S$. Obviously, the cross-sections are insensitive to the solvation energy. To demonstrate that this is generally not the case, we present in Figure 7 the cross-sections calculated with different solvation energies, but with the polarization interaction corresponding to that of the monomer. Figure 7 shows that, for a smaller polarization interaction, the solvation effect gradually destroys the VFR. From these results we conclude that for the dimer the energy dependence and the absolute magnitude of the DA cross-section

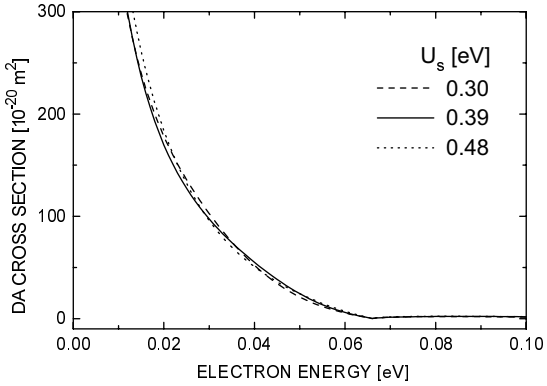


**Fig. 6.** Calculated cross-sections for dissociative electron attachment to the methyl iodide dimer, as obtained for different solvation energies in the complex $CH_3I$–$CH_3I^-$.

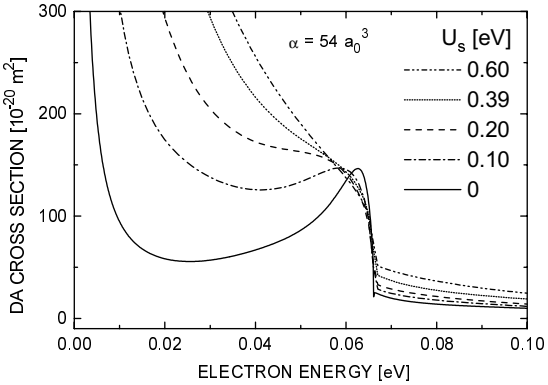


**Fig. 7.** Calculated cross-sections for dissociative electron attachment to $CH_3I$ monomers and different (model) $CH_3 + I^-$ potential curves, "solvation"-shifted by the indicated amounts from the proper $CH_3 + I^-$ curve (full curve in Fig. 4).

is dominated by the (properly treated) polarization interaction. It is interesting to compare this case with that of $N_2O$ clusters [18]. In the latter systems (ignoring geometrical considerations) the long range electron-target interactions are insufficient to promote a VFR state for a single molecule, they are, however, sufficiently strong for clusters above a certain size to give rise to VFRs (with small, but clearly observed redshifts). Moreover, the specific potential curves underlying DA to $N_2O$ clusters make the occurrence of VFRs less sensitive to changes in the long range forces. In contrast, the combination of the special curve crossing point and long range forces makes the VFRs in the methyl iodide cluster systems very susceptible to such changes, although the principal nature of the observed resonances (*i.e.* an electron weakly bound to a vibrationally excited system) is the same in both cases. We note that the cusp structure associated with the threshold for vibrational excitation of the symmetric C–I stretch at $E = 66.1$ meV is still clearly seen in Figures 6 and 7. The calculated DA cross-sections are very small above the vibrational excitation threshold, whereas the experimental cross-sections do not exhibit this behavior. This can be explained by interaction of the C–I stretch mode with other

modes in the complex. In particular, the vibrational dynamics of the complex is influenced by interaction between the I atoms in the dimer. According to Wang *et al.* [44], this interaction creates a shallow potential well in the I–I coordinate. For the most stable configuration of the system discussed above, the frequency of low-lying vibrations in this well is $2.5 \times 10^{-4}$ au ($\hbar\omega = 6.8$ meV); however, a change of the mutual orientation of two monomers leads to a fast decrease of this frequency and ultimately to a destabilization of the cluster.

To take into account these soft-mode vibrations, we consider now $R$-matrix parameters as functions of two internuclear coordinates, $\rho_1$(C–I) and $\rho_2$(I–I). We assume that the soft-mode vibrations can be described in the harmonic approximation. Moreover, we will assume harmonicity for both neutral and negative-ion states and assume the same frequency of vibrations in both states. These assumptions correspond to a widely used displaced harmonic oscillator model [47,48]. In particular, Thoss and Domcke [49,50] used this model to describe intramolecular vibrational relaxation in low-energy electron scattering and photoionization of large molecules. This model describes satisfactorily the interaction between a specific (system) vibrational mode with a background (bath) mode. Whereas the physics of this phenomenon is very similar to the physics of our problem, we use a somewhat different approach for description of the system-bath interaction, in order to make a direct connection between DA to the cluster and to the monomer.

In our approach the DA amplitudes satisfy an infinite system of algebraic equations with coefficients expressed through the matrix elements of $\gamma(\rho_1, \rho_2)$ between vibrational states of the neutral target and dissociating states of the negative ion, and through the matrix elements of $\gamma G_{\mathrm{E}} \gamma$ where $G_{\mathrm{E}}$ is the Green's function for the nuclear motion corresponding to the dissociating negative-ion state. We will assume that $\gamma$ weakly depends on $\rho_2$. In this case the modification of the matrix elements of $\gamma$ due to the bath degree of freedom is reduced to a calculation of the Franck-Condon integrals in $\rho_2$. In the displaced oscillator model they can be conveniently expressed through the Laguerre polynomials [45] as functions of the parameter

$$\Theta = (1/2)\mu\omega R_0^2 \tag{7}$$

where $\mu$ is the reduced mass corresponding to the soft-mode vibrations, $\omega$ is the frequency of these vibrations, and $R_0$ is the distance between the minima of two potential curves, describing the neutral and negative potential curves. Since we have only a rough estimate for $\omega$, and $R_0$ is not known at all, we consider $\Theta$ as a phenomenological parameter. The Green's function incorporating the soft-mode vibrations can be written as

$$G_{\mathrm{E}}(\rho_1, \rho_2, \rho_1', \rho_2') = \sum_p \psi_p(\rho_2) G^{(1)}_{\mathrm{E}-\varepsilon_p}(\rho_1, \rho_1') \psi_p(\rho_2') \tag{8}$$

where $\varepsilon_p$ and $\psi_p$, $p = 0, 1, \ldots$ are the eigenenergies and eigenstates of the harmonic Hamiltonian describing the soft-mode vibrations of the negative ion, and $G^{(1)}_{\mathrm{E}}$ is the Green's function describing the C–I motion in the dissociating state. Using (8), we can reduce the matrix elements of $G_{\mathrm{E}}$ to a sum of products of matrix elements $G^{(1)}_{\mathrm{E}}$ and Franck-Condon overlaps in $\rho_2$. After this the problem is reduced to solving a system of $N_{\mathrm{v}} N_{\mathrm{p}}$ linear algebraic equations for $N_{\mathrm{v}} N_{\mathrm{p}}$ attachment amplitudes where $N_{\mathrm{v}}$ is the number of states included to describe C–I stretch vibrations, and $N_{\mathrm{p}}$ the number of states included to describe the I–I (soft-mode) vibrations. We assume that initially the dimer is in the ground vibrational state, with respect to both the C–I vibrations and – less well justified – the soft-mode vibrations. However, in the final states many soft-mode vibrational states of the $(CH_3I)I^-$ residue are populated, and to compare with the experiment, we sum over all final vibrational states.

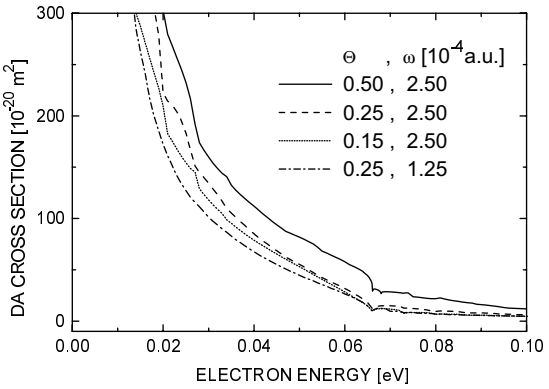


**Fig. 8.** Calculated cross-sections for dissociative electron attachment to the methyl iodide dimer, obtained with inclusion of the vibrational modes of a coupled bath system for different coupling strengths $\Theta$ (see text).

In Figure 8 we present four sets of theoretical results for the DA cross-sections involving dimers, employing three different values of the coupling parameter, $\Theta = 0.15$, 0.25, and 0.5. The further increase of $\Theta$ leads to a too rapid change of the cross-section as a function of energy. Small values of $\Theta$ lead basically to the same results as those presented in Figure 6. The curves exhibit some structure associated with threshold for excitation of the soft-mode vibrations. Three curves presented in Figure 8 include the soft-mode vibrations with frequency $\omega = 2.5 \times 10^{-4}$ au ($\hbar\omega = 6.8$ meV), the value corresponding to the stable configuration of $(CH_3I)_2$ as calculated by Wang *et al.* [44]. This should be considered as an upper bound to the actual value since the rocking vibrations destroy the stability of the I–I stretch. Other calculations with lower values of $\hbar\omega$ demonstrate basically the same behavior but with almost no structure and with slower variation of the cross-section as a function of energy which leads to better agreement with experiment. We demonstrate this by adding another curve to Figure 8 calculated with $\omega = 1.25 \times 10^{-4}$ and $\Theta = 0.25$.

In Figure 9 we compare the experimental energy dependent rate coefficient for $(CH_3I)\cdot I^-$ formation with that calculated for DA to the dimer. Figure 9 indicates that agreement between theory and experimental at the

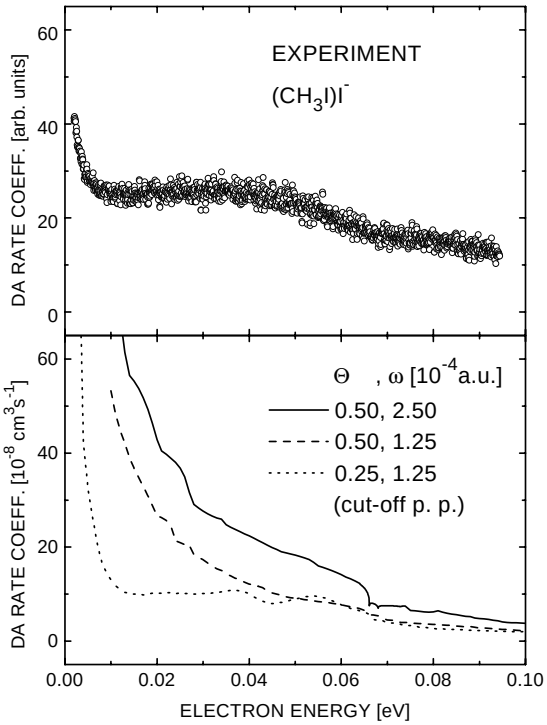


**Fig. 9.** Comparison between experimental (upper graph) and calculated rate coefficients $k_e(E)$ for dissociative electron attachment to methyl iodide dimers yielding $(CH_3I)\cdot I^-$ ions.

present stage should be considered more qualitative than quantitative: the theory confirms that the solvation and polarization effects destroy the VFR and lead to almost complete disappearance of the threshold cusp due to coupling with the bath modes. On the other hand, the theoretical rate drops with energy too fast as compared to the experimental observation. Although the theoretical data are presented for values of $\Theta$ and $\omega$ which are not fully optimized, attempts to optimize them did not lead to substantially better agreement.

We should stress that due to the lack of detailed information about the geometrical and electronic structure of the methyl iodide dimer, our theory contains too many model assumptions to expect quantitative agreement: in particular, our polarization model discussed in Section 3.3 is very approximate and is likely to overestimate polarization interaction between the electron and the dimer. To correct for this flaw of our model, we can introduce a polarization potential $-\alpha/[2(r^2+r_c^2)^2]$ with a phenomenological parameter $r_c$ which cuts off the polarization attraction at short distances. theb In Figure 9 we also present the rate coefficients calculated for $\Theta = 0.25$, $\omega = 1.25 \times 10^{-4}$ au and $r_c = 6.75a_0$ which give much better agreement with the experimental values. In particular the plateau behavior between 10 and 40 meV can be reproduced quite well, although we observe some structure associated with the coupling with the bath modes and with the $\nu_3 = 1$ threshold. However, this structure is not stable with respect to variation of the parameters $\omega$, $\Theta$ and $r_c$ and therefore should not be considered as real: for its accurate calculation we need more information about the bath mode and its interaction with the C–I stretch mode responsible for dissociative attachment. On the other hand, the cross-section averaged over this structure is stable for a given cut-off parameter $r_c$. Since this structure is more pronounced in calculations with the polarization cut-off, we conclude that a strong polarization interaction suppresses it.

## 4 Conclusions

In the present work we have studied electron attachment to methyl iodide clusters and have found strong influence of clustering on the DA process: whereas a prominent vibrational Feshbach resonance (VFR) below the onset for the C–I stretch vibration is observed for DA to monomers, only weak and broad structure, shifted to lower energies, is detected for formation of $(CH_3I)\cdot I^-$ and essentially no structure is left in production of $(CH_3I)_2\cdot I^-$. The results of our model $R$-matrix calculations which fully describe the VFR in the monomer, do not provide quantitative explanation of the rate coefficient observed for the $(CH_3I)\cdot I^-$ anion. However, they allow us to conclude that two mechanisms are responsible for the disappearance of the vibrational Feshbach resonance: shift of the negative-ion curve due to solvation (including modification of the long-range electron-molecule interaction) and interaction with soft-mode vibrations which not only destroy the resonance, but also smear out the pronounced cusp structure at the $\nu_3 = 1$ threshold observed in DA to the monomer.

This work was supported by the Deutsche Forschungsgemeinschaft (Schwerpunktprogramm *Molekulare Cluster* and Forschergruppe *Niederenergetische Elektronenstreuprozesse*), by the Graduiertenkolleg *Laser- und Teilchenspektroskopie* and through the Zentrum für Lasermeßtechnik und Diagnostik. We gratefully acknowledge L.S. Cederbaum, M.A. Johnson and C.E. Dessent for helpful discussions, and G.A. Gallup for providing his quantum chemistry results for the methyl iodide dimer prior to publication. IIF thanks the members of the Forschergruppe for their hospitality during his stay at Fachbereich Physik, Universität Kaiserslautern, and the US National Science Foundation for support through grant PHY-9801871.

## References

1. T.D. Märk, Int. J. Mass Spectrom. Ion Proc. **107**, 143 (1991).
2. *Clusters of Atoms and Molecules*, edited by H. Haberland (Springer Series in Chemical Physics, Springer-Verlag, Berlin, Heidelberg, 1994), Vol. 56.
3. O. Ingolfsson, F. Weik, E. Illenberger, Int. J. Mass Spectrom. Ion Proc. **155**, 1 (1996).
4. A.W. Castleman Jr, K.H. Bowen Jr, J. Phys. Chem. **100**, 12911 (1996).
5. J.V. Coe, A.D. Earhardt, M.H. Cohen, G.J. Hoffman, H.W. Sarkas, K.H. Bowen, J. Chem. Phys. **107**, 6023 (1997).
6. C.E. Dessent, J. Kim, M.A. Johnson, Acc. Chem. Res. **31**, 527 (1998).

7. G. J. Schulz, Rev. Mod. Phys. **45**, 423 (1973).
8. R.N. Compton, in *Electronic and Atomic Collisions*, edited by N. Oda, K. Takayanagi (North Holland, Amsterdam, 1980), p. 251.
9. *Electron-molecule interactions and their applications*, edited by L.G. Christophorou (Academic Press, New York, 1984), Vols. 1 and 2.
10. Y. Hatano, in *Electronic and Atomic Collisions*, edited by D.C. Lorents, W.E. Meyerhof, J.R. Peterson (North Holland, Amsterdam, 1986), p. 153.
11. M. Allan, J. Electron Spectrosc. Rel. Phen. **48**, 219 (1989).
12. J. Bardsley, F. Mandl, Rep. Prog. Phys. **31**, 501 (1968).
13. J.P. Gauyacq, A. Herzenberg, Phys. Rev. A **25**, 2959 (1982).
14. W. Domcke, L.S. Cederbaum, J. Phys. B **14**, 149 (1981).
15. G. Knoth, M. Gote, M. Rädle, K. Jung, H. Ehrhardt, Phys. Rev. Lett. **62**, 1735 (1989).
16. A. Schramm, I.I. Fabrikant, J.M. Weber, E. Leber, M.-W. Ruf, H. Hotop, J. Phys. B **32**, 2153 (1999).
17. C.E.H. Dessent, C.G. Bailey, M.A. Johnson, J. Chem. Phys. **105**, 10416 (1996).
18. J.M. Weber, E. Leber, M.-W. Ruf, H. Hotop, Phys. Rev. Lett. **82**, 516 (1999).
19. E. Leber, I.I. Fabrikant, J.M. Weber, M.-W. Ruf, H. Hotop, in *Dissociative Recombination: Theory, Experimental and Application IV*, edited by M. Larsson, J.B.A. Mitchell, I.F. Schneider (World Scientific, Singapore, 2000), pp. 69–76.
20. T.D. Märk, K. Leiter, W. Ritter, A. Stamatovic, Phys. Rev. Lett. **55**, 2559 (1985).
21. S. Matejcik, A. Kiendler, P. Stampfli, A. Stamatovic, T.D. Märk, Phys. Rev. Lett. **77**, 3771 (1996).
22. S. Matejcik, P. Stampfli, A. Stamatovic, P. Scheier, T.D. Märk, J. Chem. Phys. **111**, 3548 (1999).
23. M. Knapp, O. Echt, D. Kreisle, E. Recknagel, J. Chem. Phys. **85**, 636 (1986).
24. J.M. Weber, E. Leber, M.-W. Ruf, H. Hotop, Eur. Phys. J. D **7**, 587 (1999).
25. S.H. Alajajian, M.T. Bernius, A. Chutjian, J. Phys. B **21**, 4021 (1988).
26. C.E. Klots, R.N. Compton, Chem. Phys. Lett. **73**, 589 (1980).
27. D.M. Cyr, G.A. Bishea, M.G. Scarton, M.A. Johnson, J. Chem. Phys. **97**, 5911 (1992).
28. D.M. Cyr, M.G. Scarton, M.A. Johnson, J. Chem. Phys. **99**, 4869 (1993).
29. D.M. Cyr, C.G. Bailey, D. Serxner, M.G. Scarton, M.A. Johnson, J. Chem. Phys. **101**, 10507 (1994).
30. C.C. Arnold, D.M. Neumark, D.M. Cyr, M.A. Johnson, J. Phys. Chem. **99**, 1633 (1995).
31. D. Klar, M.-W. Ruf, H. Hotop, Chem. Phys. Lett. **189**, 448 (1992); Aust. J. Phys. **45**, 263 (1992).
32. D. Klar, M.-W. Ruf, H. Hotop, Meas. Sci. Technol. **5**, 1248 (1994).
33. A. Schramm, J.M. Weber, J. Kreil, D. Klar, M.-W. Ruf, H. Hotop, Phys. Rev. Lett. **81**, 778 (1998).
34. E.P. Wigner, Phys. Rev. **73**, 1002 (1948).
35. I.I. Fabrikant, Sov. Phys. JETP **46**, 693 (1977).
36. W. Domcke, Phys. Rep. **208**, 97 (1991).
37. H. Hotop, D. Klar, J. Kreil, M.-W. Ruf, A. Schramm, J.M. Weber, in *The Physics of Electronic and Atomic Collisions*, edited by L.J. Dube, J.B.A. Mitchell, J.W. McConkey, C.E. Brian (AIP Conf. Proc. **360**, AIP, New York, 1995), p. 267.
38. C.W. Walter, B.G. Lindsay, K.A. Smith, F.B. Dunning, Chem. Phys. Lett. **154**, 409 (1989).
39. J. Bertran, I. Gallardo, M. Moreno, J.-M. Saveant, J. Am. Chem. Soc. **114**, 9576 (1992).
40. *CRC Handbook of Chemistry and Physics*, edited by D.R. Lide, 76th edn. (CRC press, Boca Raton, USA, 1994–1995).
41. T. Shimanouchi, *Tables of molecular frequencies*, NSRDS(NBS) **1**, 39 (1972).
42. D. Hanstorp, M. Gustafsson, J. Phys. B **25**, 1773 (1992).
43. J.F. Ogilvie, W.R. Rodwell, R.H. Tipping, J. Chem. Phys. **96**, 2061 (1980).
44. P.G. Wang, Y.P. Zhang, C.J. Ruggles, L.D. Ziegler, J. Chem. Phys. **92**, 2806 (1990).
45. M. Ehbrecht, A. de Meijere, M. Stemmler, F. Huisken, J. Chem. Phys. **97**, 3021 (1992).
46. G.A. Gallup, private communication (1999).
47. W. Domcke, L.S. Cederbaum, Phys. Rev. A **16**, 1465 (1977).
48. G.V. Golubkov, F.I. Dalidchik, K.K. Ivanov, Zh. Eksp. Teor. Fiz. **73**, 439 (1977); Sov. Phys. JETP **46**, 230 (1977).
49. M. Thoss, W. Domcke, J. Chem. Phys. **106**, 3174 (1997).
50. M. Thoss, W. Domcke, J. Chem. Phys. **109**, 6577 (1998).